

Angiotensin-(1-7) Modulates the Warburg Effect to Alleviate Inflammation in LPS-Induced Macrophages and Septic Mice

Dan Yu , Wenhan Huang, Min Sheng, Shan Zhang, Hang Pan, Feifeng Ren, Lei Luo, Jun Zhou, Dongmei Huang, Lin Tang

Department of Rheumatology and Immunology, Second Affiliated Hospital of Chongqing Medical University, Chongqing, People's Republic of China

Correspondence: Lin Tang, Department of Rheumatology and Immunology, Second Affiliated Hospital of Chongqing Medical University, 74 Linjiang Road, Yuzhong District, Chongqing, People's Republic of China, Tel +86 23 63693878, Fax +86 23 62888265, Email hopetang@hospital.cqmu.edu.cn

Purpose: Inflammation triggers a metabolic shift in macrophages from oxidative phosphorylation to glycolysis, a phenomenon known as the Warburg effect. This metabolic reprogramming worsens inflammation and cascades into organ damage. Angiotensin-(1-7) [Ang-(1-7)], a small molecule, has demonstrated anti-inflammatory properties. This study investigates whether Ang-(1-7) mitigates inflammation in LPS-induced macrophages and septic mice by regulating the Warburg effect in immune metabolism.

Methods: The study induced macrophages with LPS in vitro and measured inflammatory factors using ELISA and Western blot. Key enzymes in glycolysis, mitochondrial respiratory complexes, and citrate pathway key molecules were assessed using Western blot and qRT-PCR. Mitochondrial membrane potential (MMP), lactate, and ATP were measured using assay kits. In vivo, a mouse model of sepsis induced by LPS was used. Kidney tissues were examined for pathological and mitochondrial ultrastructural alterations. The levels of inflammatory factors in mouse serum, glycolysis and citrate pathway-related molecules in the kidney were assessed using qRT-PCR, Western blot, and immunofluorescence techniques. Additionally, MMP, lactate, and ATP in the kidney were measured using assay kits.

Results: In vitro experiments demonstrated that Ang-(1-7) inhibited the levels of inflammatory factors in LPS-treated RAW264.7 cells. It also reduced the expression of key glycolytic enzymes HK2, PFKFB3, and PKM2, as well as lactate levels. Additionally, it decreased intracellular citrate accumulation, enhanced mitochondrial respiratory complexes I and III, and ATP levels. Ang-(1-7) alleviated MMP damage, modulated citrate pathway-related molecules, including SLC25A1, ACLY, and HIF-1 α . In vivo experiments showed that Ang-(1-7) lowered glycolysis levels in septic mice, improved mitochondrial ultrastructure and function, mitigated inflammation and renal tissues damage in septic mice, and suppressed the expression of key molecules in the citrate pathway.

Conclusion: In conclusion, Ang-(1-7) can regulate the Warburg effect through the citrate pathway, thereby alleviating inflammation in LPS-induced macrophages and septic mice.

Keywords: Ang-(1-7), macrophage, sepsis, Warburg effect, glycolysis, citrate

Introduction

Sepsis is a systemic exaggerated inflammatory response to infection or injury, leading to multi-organ dysfunction.¹ One of the key factors in sepsis is the excessive activation and immune metabolic dysregulation of macrophages.² Macrophages in sepsis produce pro-inflammatory cytokines, which initiate the innate immune response.³ Meanwhile, there is a significant shift in the immune metabolism pattern of macrophages, particularly in the alteration of glucose metabolism.⁴ The core metabolism of macrophages shifts from oxidative phosphorylation (OXPHOS) to aerobic glycolysis, a change referred to as the Warburg effect.⁵

The Warburg effect plays a crucial role in inflammation. Macrophages activated by LPS shift their cellular metabolism towards the glycolytic pathway to fulfill the rapid increase in energy demands required for synthesizing inflammatory factors.⁶⁻⁸ The glycolysis process further triggers the inflammatory response in macrophages. The key rate-

limiting enzyme in glycolysis, such as pyruvate kinase M2 (PKM2), is a critical determinant in the activation of macrophages by LPS, promoting the production of inflammatory factors and triggering the inflammatory response.⁹ However, during inflammation, compared to enhanced glycolysis, the activity of the tricarboxylic acid (TCA) cycle in the mitochondria decreases, OXPHOS is inhibited, and ATP production is reduced.¹⁰ This impairment affects the immune function of activated macrophages, rendering them unable to meet their energy requirements.

The ATP generated by the mitochondrial TCA cycle is the primary source of cellular energy.¹¹ However, under inflammatory condition, the TCA cycle is interrupted, leading to citrate accumulation.¹² Citrate serve as an inflammatory signaling molecule in macrophages.¹³ It enters the cytoplasm through the mitochondrial citrate carrier, SLC25A1,¹⁴ and is then cleaved by ATP-citrate lyase (ACLY). This activation of the mitochondrial citrate export pathway involved in inducing glycolysis.^{15,16} Studies have confirmed that citrate export pathway promotes hypoxia-inducible factor-1 α (HIF-1 α) dependent gene transcription.^{17,18} HIF-1 α plays a significant role in altering glucose metabolism by activating key enzymes in glycolysis and affecting the stability of mitochondrial respiratory complexes.^{19–21} Therefore, regulating the SLC25A1-HIF-1 α pathway may help suppress the Warburg effect, thereby reducing inflammation and protecting organs.

A growing body of evidence suggests that the Ang-(1-7)/Mas axis, a component of renin-angiotensin-aldosterone system (RAAS), confers protective effects, such as anti-inflammatory, anti-oxidative, and anti-fibrotic effects.^{22,23} Our preliminary research has indicated that Ang-(1-7) can inhibit the inflammatory response in macrophages and septic mice.²⁴ However, the specific regulatory mechanism remains unclear. Therefore, this study aims to further explore whether Ang-(1-7) alleviates inflammation in LPS-induced macrophages and septic mice by modulating the Warburg effect.

Materials and Methods

Cell Culture and Treatments

RAW264.7 cells were obtained from the American Type Culture Collection (Manassas, VA, USA) and cultured in high-glucose DMEM medium (Gibco, Waltham, MA, USA) supplemented with 10% fetal bovine serum and 1% penicillin-streptomycin. The cells were maintained in a constant temperature cell culture incubator at 37°C with 5% CO₂. Utilizing previously published data,²⁴ a cellular model was constructed using lipopolysaccharide (LPS) (Sigma-Aldrich, St. Louis, MO, USA) at a concentration of 1 μ g/mL. Initially, the cells were pre-treated with A-779 (MedChemExpress, USA) at a concentration of 10⁻⁵ mol/L for 30 minutes, followed by intervention with Ang-(1-7) (MedChemExpress, USA) at a concentration of 10⁻⁶ mol/L. The cells were cultured for 24 hours in the presence or absence of LPS.

Cell Viability Assay

The cell viability was analyzed using the Cell Counting Kit-8 (Dojindo, Kumamoto, Japan). RAW264.7 cells were seeded at a density of 5000 cells per well in a 96-well plate and incubated overnight. After drug treatment, 10 μ L of CCK-8 solution was added to each well and incubated in a cell culture incubator. Subsequently, the absorbance at 450 nm was measured using a microplate reader (Thermo Fisher Scientific, USA) to calculate cell viability. Cell viability (%) was calculated using the following formula: cell viability (%) = (experimental group absorbance-blank group absorbance)/(control group absorbance-blank group absorbance) \times 100%.

Animals

All experimental procedures involving mice were approved by the Chongqing Medical University Animal Ethics Committee and conducted in accordance with the Chongqing Medical University Animal Experiment Guidelines. C57BL/6 male mice (8–10 weeks old) were purchased from the Experimental Animal Center of Chongqing Medical University. Sepsis was induced in the mice by intraperitoneal injection of LPS. All animals were randomly divided into three groups (n=8 per group): control group, LPS group, and LPS+Ang-(1-7) group. The animals in the LPS+Ang-(1-7) group were injected with Ang-(1-7) (2 mg/kg) daily for three consecutive days. The control group and the LPS group were injected with the same volume of saline solution. After three days, both the LPS group and the LPS+Ang-(1-7)

group were injected with LPS (10 mg/kg) within 30 minutes. After 24 hours of LPS injection, mouse kidney tissues and blood samples were collected for experimentation.

Enzyme-Linked Immunosorbent Assay (ELISA)

The levels of TNF- α and IL-6 in cell culture supernatant and mouse serum were detected using an ELISA kit (Jiubang Biotechnology, Quanzhou, China). The ELISA kit was equilibrated to room temperature, standard wells and sample wells were prepared, and standards, samples, and reagents were added according to the instructions. Finally, the absorbance at 450 nm was measured, and the sample concentrations were calculated according to the instructions manual.

Western Blot Analysis

RAW264.7 cells and kidney tissues were collected and added with RIPA lysis buffer (Beyotime, Shanghai, China). After thorough lysis on ice, the lysates were centrifuged at 4°C, and the supernatants were collected. The concentration of total proteins in the supernatant was determined using the BCA protein assay kit (Solarbio, Beijing, China). Equal amounts of protein were separated using SDS-PAGE and transferred onto PVDF membranes (Millipore Sigma, Burlington, MA, USA). The membranes were blocked at room temperature for 60 minutes and then incubated overnight at 4°C with the corresponding primary antibodies. Afterwards, the corresponding species-specific secondary antibodies (Proteintech, Wuhan, China) were incubated on a shaker at room temperature for 60 minutes. Finally, ECL Western Blot Substrates (Zenbio, Chengdu, China) were applied to the protein bands, and chemiluminescent signals were detected using imaging equipment. All antibodies used for Western blot analysis are as follows: β -actin (20,536-1-AP, Proteintech), TNF- α (17,590-1-AP, Proteintech), IL-6 (12,912, Cell Signaling Technology), SLC25A1 (15,235-1-AP, Proteintech), HK2 (22,029-1-AP, Proteintech), PFKFB3 (13,763-1-AP, Proteintech), PKM2 (15,822-1-AP, Proteintech), NDUFB8 (14,794-1-AP, Proteintech), UQCERS1 (18,443-1-AP, Proteintech), ACLY (ab40793, Abcam), HIF-1 α (ab179483, Abcam).

Quantitative Real-Time PCR (qRT-PCR)

Total RNA from cells or tissues was extracted using the SteadyPure Quick RNA Extraction Kit (Accurate Biology, Hunan, China). The concentration and purity of the extracted RNA samples were determined. Afterwards, the extracted RNA was reverse-transcribed into cDNA using RT Master Mix for qPCR II (MedChemExpress, USA). Subsequently, qRT-PCR reactions were performed using SYBR Green qPCR Master Mix (MedChemExpress, USA) and the CFX96 RT-PCR system (Bio-Rad, USA). Finally, quantitative data analysis was conducted using the $2^{-\Delta\Delta C_t}$ method. Primer sequences are listed in Table 1.

Table 1 Sequences of Primers Used for the qRT-PCR

Genes	Forward (5'- 3')	Reverse (5'- 3')
β -actin	CATCCGTAAAGACCTCTATGCCAAC	ATGGAGCCACCGATCCACA
Slc25a1	AGATGAACGAGCGAACCCAC	GATGGAGCCGTAGAGCAAGG
Acly	TAGGACAGCATCTTTTTCTGAGT	GACTTGGGACTGAATCTTGGG
HIF-1 α	CTTTACCAACTCAAACAGTCCC	CAGGGTGGGCAGAACATTTA
Hk2	CGGAGTTGTTCTGCTTTGGA	TCACTGGGTCACTAAGGCTC
Pfkfb3	GCCTCTTGACCCTGATAAATGTG	ATTCGGCTCTGGATGTGGT
Pkm2	AAACAGCCAAGGGGGACTAC	AACAGCAGACGGTGAACAT

Assays of Lactate and Citrate Content

Lactate content was measured using the lactate assay kit (Jiancheng Bioengineering Institute, Nanjing, China). Lactate content was calculated according to the instruction manual. Citrate content in cells was determined using the citrate assay kit (Jiancheng Bioengineering Institute, Nanjing, China) following the kit instructions.

Mitochondrial Membrane Potential (MMP) Assay

The MMP levels in cells and kidney tissues were assessed using the JC-1 staining kit (Beyotime, Shanghai, China). For cellular MMP detection, cells were evenly seeded in six-well plates. JC-1 staining working solution was added following the instructions provided with the kit. After incubation, cells were washed with JC-1 staining buffer. The samples were observed under a fluorescence microscope to distinguish JC-1 monomers (green fluorescence) and JC-1 polymers (red fluorescence). MMP in kidney tissues was assessed using the following method. Firstly, kidney tissues were processed using a tissue mitochondrial isolation kit (Beyotime, Shanghai, China) to extract mitochondrial organelles. The total protein concentration in the mitochondrial samples was determined using the BCA protein quantification method. Subsequently, purified mitochondria were suspended in diluted JC-1 working solution. Finally, the fluorescence intensity values of JC-1 polymers and monomers were measured using a fluorescence microplate reader. Calculate the ratio of JC-1 polymers and monomers.

ATP Content Detection

The ATP content in cells and kidney tissues was determined using an ATP assay kit (Beyotime, Shanghai, China). According to the manufacturer's instructions, cells or tissues were lysed with lysis buffer after centrifugation, and the supernatant was collected. ATP detection working solution was added to the wells, followed by the addition of samples or standard solutions. The mixture was swiftly mixed and then the relative light units (RLU) were measured using an enzyme-linked immunosorbent assay reader. ATP content was calculated based on the instructions provided.

Renal Function Measurement

The blood urea nitrogen (BUN) levels and serum creatinine (Scr) levels were measured using urea nitrogen test kits and creatinine assay kits (Jiancheng Bioengineering Institute, Nanjing, China). The experimental procedures outlined in the instruction manual were followed to determine the blood urea nitrogen and creatinine content.

Hematoxylin–Eosin (HE) Staining

The mouse kidney tissues specimens were fixed in 4% paraformaldehyde. Sections from each group were dehydrated using alcohol gradients, embedded in paraffin, and cut into thin slices measuring 5 μ m. These sections were stained with hematoxylin-eosin (HE) and observed under a light microscope to assess the histopathological differences in kidney tissues.

Immunofluorescence Staining

Tissue sections were sequentially incubated in xylene and different concentrations of ethanol. Antigen retrieval was performed using microwave treatment, followed by blocking with 5% BSA at room temperature for 60 minutes. Subsequently, the sections were incubated overnight at 4°C with an appropriately diluted primary antibody. After the tissue sections were rewarmed the next day, they were incubated with an appropriately diluted secondary antibody specific to the corresponding species (Proteintech, Wuhan, China) at room temperature in the dark for 60 minutes. Finally, nuclear staining was performed using DAPI staining solution (Beyotime, Shanghai, China), and the slides were sealed with anti-fade mounting medium to prevent fluorescence quenching. Samples were analyzed using a fluorescence microscope (Nikon, Tokyo, Japan), and microscopic images were obtained.

Transmission Electron Microscopy (TEM)

The kidney tissues were sliced into 1 mm³ sections using sterile blades. The tissues were fixed in 4% glutaraldehyde and stained with 1% osmium tetroxide. Subsequently, dehydration was carried out in ascending concentrations of acetone, followed by embedding in epoxy resin. Ultrathin sections were cut and stained with uranyl acetate and lead citrate. The ultrastructure of mitochondria in kidney tissues was observed under an electron microscope (Hitachi H7500 TEM, Tokyo, Japan).

Results

Ang-(1-7) Suppressed the Inflammatory Response in LPS-Induced RAW264.7 Cells

LPS, the primary component of bacterial endotoxin, induces severe inflammatory responses in macrophages. Therefore, we utilized an LPS-stimulated macrophage model to investigate the anti-inflammatory activity of Ang-(1-7) in vitro. Using CCK-8 assay to measure cell viability, it was observed that LPS, Ang-(1-7), and/or A-779 did not exhibit significant cytotoxic effects on RAW264.7 cells compared to the control group (Figure 1A). Under LPS stimulation, the levels of inflammatory cytokines TNF- α and IL-6 in the supernatant of RAW264.7 cells cultures were significantly elevated. After Ang-(1-7) treatment, the levels of TNF- α and IL-6 were markedly reduced compared to the LPS-

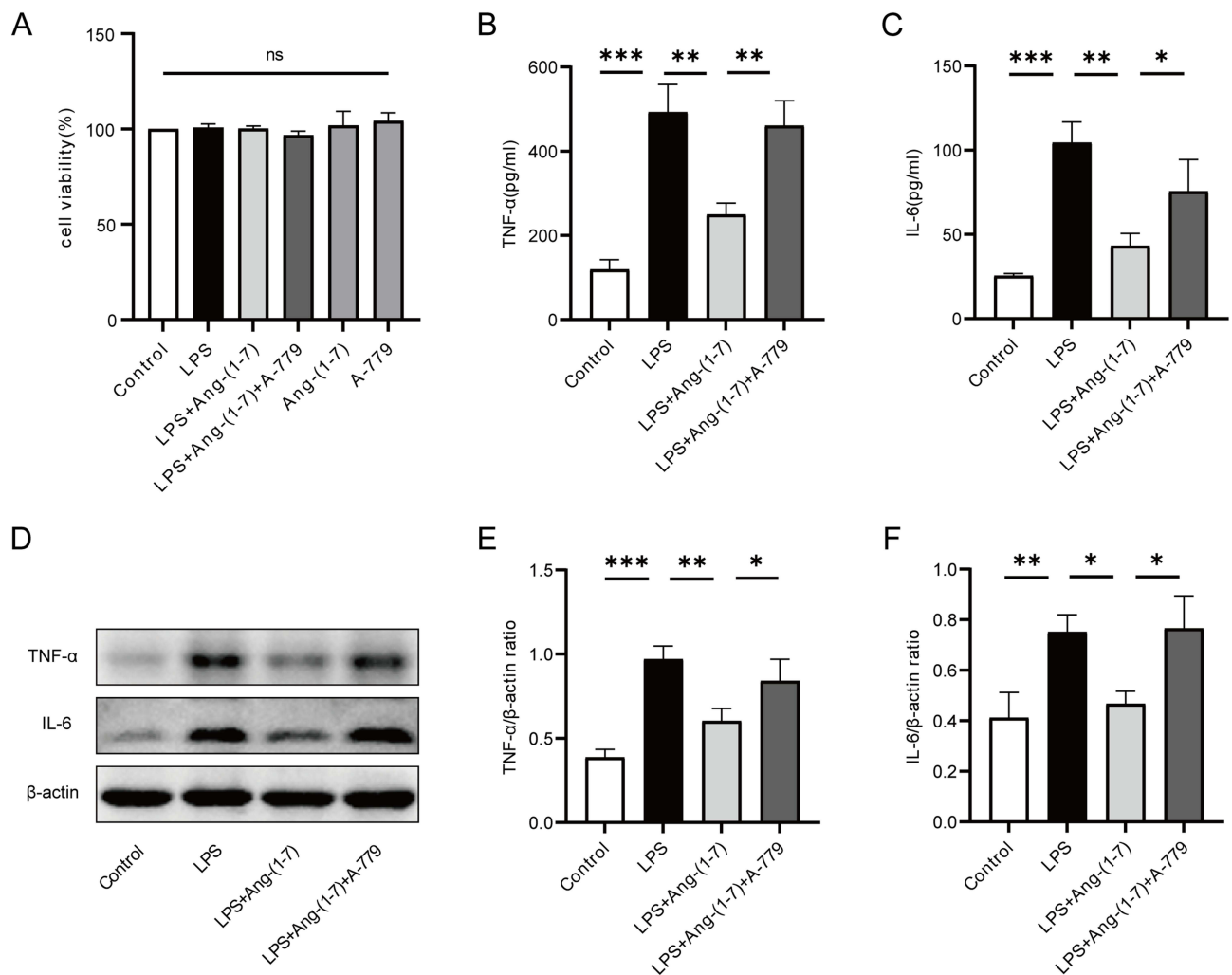


Figure 1 Ang-(1-7) mitigated the secretion of inflammatory cytokines in LPS-induced RAW264.7 cells. **(A)** Cell viability of RAW264.7 cells was assessed using the CCK-8 assay. **(B and C)** Levels of TNF- α and IL-6 in the cell culture supernatant of RAW264.7 cells were measured using ELISA. **(D)** Protein expression of TNF- α and IL-6 was detected using Western blot analysis. **(E and F)** Quantification of protein concentrations for TNF- α and IL-6. Error bars indicated the mean \pm SD for three separate experiments, ns: non-significant, * p < 0.05, ** p < 0.01, *** p < 0.001.

stimulated group. While A-779, acting as a Mas receptor antagonist, effectively blocked the actions of Ang-(1-7) (Figure 1B and C). Similarly, Ang-(1-7) significantly reduced the protein expression of TNF- α and IL-6 in RAW264.7 cells induced by LPS, and these effects of Ang-(1-7) were antagonized by A-779 (Figure 1D–F). These results indicate that Ang-(1-7) can inhibit the inflammatory response of macrophages after LPS stimulation through the Mas receptor.

Ang-(1-7) Inhibited the Glycolytic Levels and Ameliorated Mitochondrial Function in LPS-Induced RAW264.7 Cells

In the inflammatory state, activated macrophages shift their glucose metabolism from OXPHOS to glycolysis. Intracellular glucose is converted to pyruvate through glycolytic enzymes and further transformed into lactate, meeting the high energy demands of the cells. Western blot and qRT-PCR results revealed that, compared to the control group, LPS induction in RAW264.7 cells significantly enhanced the protein and mRNA expression of key glycolytic enzymes, hexokinase 2 (HK2), fructose-2,6-bisphosphatase 3 (PFKFB3), and PKM2. In contrast, the protein and mRNA levels of HK2, PFKFB3, and PKM2 in the Ang-(1-7) treatment group were markedly lower than those in the LPS group. Additionally, A-779 counteracted the effects of Ang-(1-7) (Figure 2A–G). Furthermore, Ang-(1-7) significantly decreased the lactate content in the cell culture supernatant after LPS stimulation, and the action of Ang-(1-7) was blocked by A-779 (Figure 2H). These results indicate that Ang-(1-7) can suppress the glycolytic levels of macrophages after LPS stimulation through the Mas receptor.

The OXPHOS metabolic pathway generates ATP by transferring electrons through a series of respiratory complexes in the inner mitochondrial membrane. To further investigate the impact of Ang-(1-7) on LPS-stimulated RAW264.7 mitochondria, alterations in mitochondrial respiratory complexes were examined using the Western blot method. The results revealed that, compared to the control group, intervention with LPS significantly reduced the expression of mitochondrial respiratory complex I (NDUFB8) and complex III (UQCRCF1) proteins. However, Ang-(1-7) markedly elevated the expression of these proteins in the LPS group, and these effects of Ang-(1-7) were blocked by A-779 (Figure 2I–K). Additionally, fluorescence microscopy analysis revealed a significant decrease in MMP levels after LPS stimulation. Interestingly, Ang-(1-7) demonstrated a remarkable increase in MMP levels within the LPS-treated group (Figure 2L and M). Similarly, Ang-(1-7) significantly increased ATP levels, while A-779 inhibited its effects (Figure 2N). These results indicate that Ang-(1-7) can restore mitochondrial respiratory complex protein levels and mitochondrial damage in macrophages stimulated by LPS, thereby improving mitochondrial function.

Ang-(1-7) Suppressed SLC25A1-HIF-1 α Expression in LPS-Induced RAW264.7 Cells

SLC25A1 exports citrate from mitochondria, subsequently cleaved by ACLY, enhancing the binding of HIF-1 α to glycolytic gene promoters, thereby promoting glycolysis and inflammatory responses. We assessed the impact of Ang-(1-7) on the expression of SLC25A1 and its downstream key proteins. Western blot analysis revealed a significant increase in SLC25A1 and ACLY protein expression in RAW264.7 cells after LPS stimulation. However, Ang-(1-7) significantly downregulated the protein expression of SLC25A1 and ACLY (Figure 3A–C). Furthermore, Ang-(1-7) significantly reduced the accumulation of citrate in LPS-stimulated RAW264.7 cells (Figure 3E). Additionally, Ang-(1-7) effectively attenuated the increased mRNA expression of SLC25A1 and ACLY in the LPS group, and these effects of Ang-(1-7) mentioned above were blocked by A-779 (Figure 3F and G). The research demonstrates that Ang-(1-7) can improve intracellular metabolic levels by reducing the accumulation of citrate within the cells via the SLC25A1 citrate pathway. We further evaluated the expression of the downstream transcription factor HIF-1 α . Ang-(1-7) significantly decreased both HIF-1 α protein and mRNA levels induced by LPS, while A-779 counteracted the effects of Ang-(1-7) (Figure 3A, D and H). These results indicate that Ang-(1-7) can modulate the Warburg effect by downregulating the expression of SLC25A1, ACLY, and HIF-1 α in LPS-induced macrophages through the Mas receptor.

Ang-(1-7) Alleviated Systemic Inflammatory Response and Kidney Injury in Septic Mice

Sepsis frequently leads to multiple organ dysfunction, with the kidney commonly affected. Concurrently, the presence of acute kidney injury in sepsis serves as an independent risk factor in predicting mortality among septic patients.²⁵ Hence, assessing

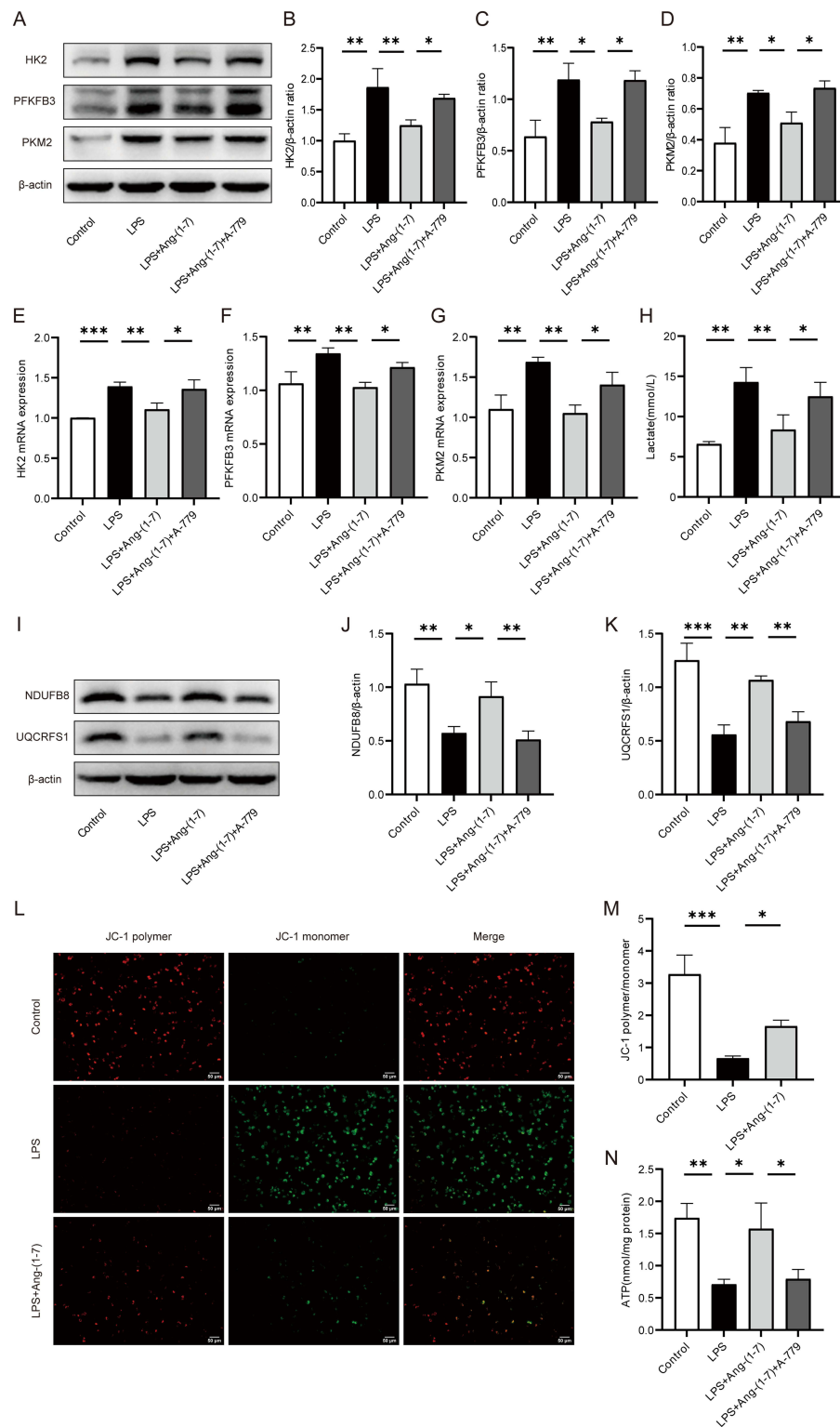


Figure 2 Ang-(1-7) alleviated LPS-induced glycolytic enzymes and lactate levels in RAW264.7 cells, and improved mitochondrial function. **(A)** Protein expression levels of glycolytic enzymes HK2, PFKFB3, and PKM2 were determined using Western blot analysis. **(B–D)** Quantification of protein concentrations for HK2, PFKFB3, and PKM2. **(E–G)** mRNA levels of HK2, PFKFB3, and PKM2 were assessed using qRT-PCR method. **(H)** Lactate levels in the cell supernatant were measured using a lactate assay kit. **(I)** Expression level of mitochondrial respiratory complex proteins NDUFB8 and UQCRCF1 was determined through Western blot analysis. **(J and K)** Quantification of protein concentrations for NDUFB8 and UQCRCF1 was performed. **(L)** Mitochondrial membrane potential was assessed using JC-1 staining. Representative images of RAW264.7 cell mitochondrial membrane potential were captured under a microscope ($\times 200$, scale bar: 50 μm). JC-1 polymer exhibited red fluorescence indicating normal mitochondrial membrane potential, while JC-1 monomer displayed green fluorescence indicating membrane potential decline. **(M)** Quantify the membrane potential levels by calculating the JC-1 polymer/monomer ratio. **(N)** ATP levels in RAW264.7 cells were determined using an ATP assay kit. Error bars indicated the mean \pm SD for three separate experiments, * $p < 0.05$, ** $p < 0.01$, *** $p < 0.001$.

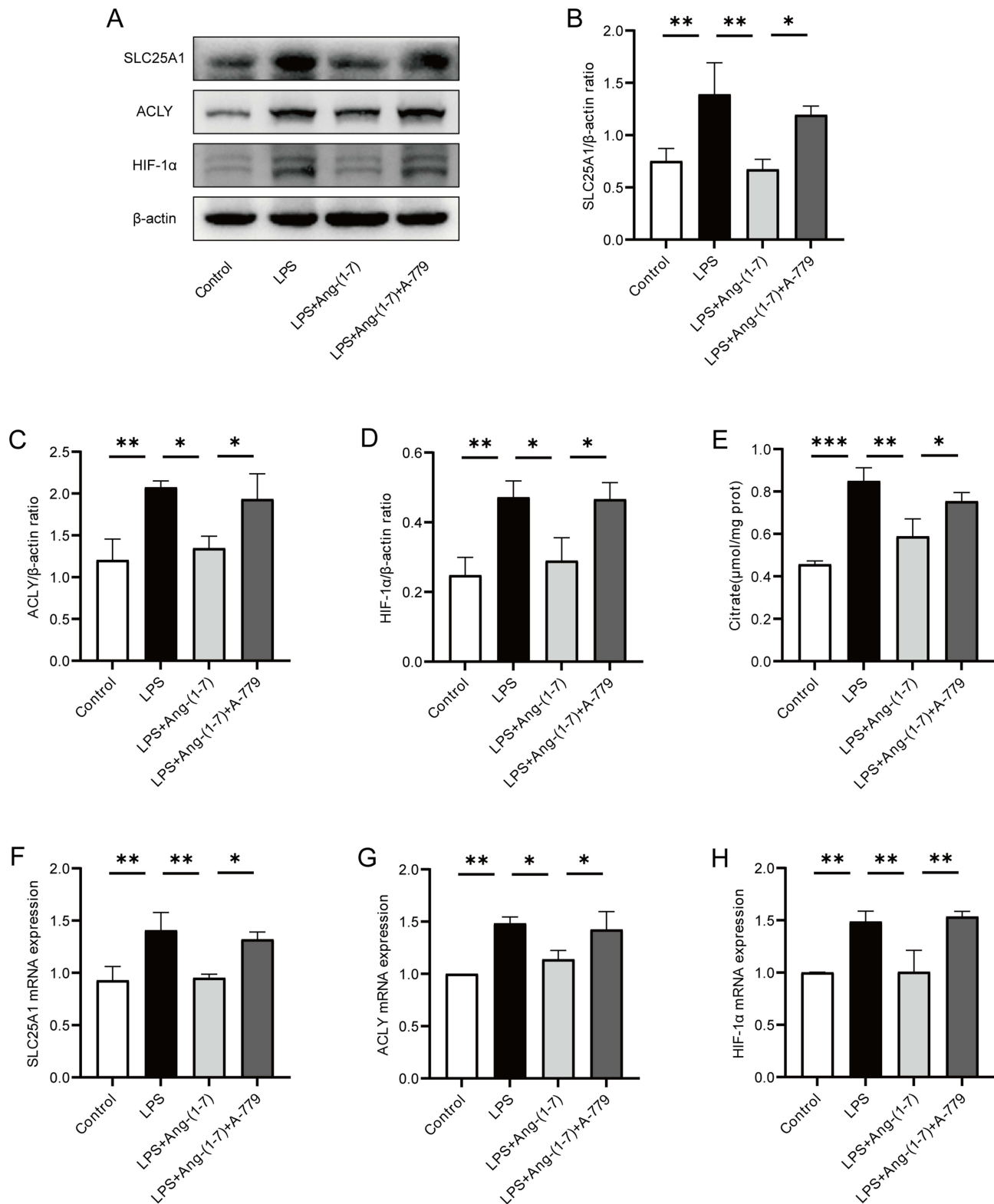


Figure 3 Ang-(1-7) inhibited the expression of SLC25A1, ACLY, and HIF-1α in the citrate output pathway of LPS-induced RAW264.7 cells. **(A)** Protein expression levels of SLC25A1, ACLY, and HIF-1α were examined using Western blot analysis. **(B–D)** Quantification of protein concentrations for SLC25A1, ACLY, and HIF-1α. **(E)** Cellular citrate levels were measured using a citrate content assay kit. **(F–H)** mRNA levels of SLC25A1, ACLY, and HIF-1α were determined using qRT-PCR method. Error bars indicated the mean ± SD for three separate experiments, *p < 0.05, **p < 0.01, ***p < 0.001.

renal function and histological changes is of paramount importance in evaluating the severity of sepsis. In this study, in order to further evaluate the impact of Ang-(1-7) on the inflammatory storm and target organs in septic mice, we utilized a septic mouse model induced by intraperitoneal injection of LPS. The kidney was selected as the target organ for further investigation. In the mouse model of sepsis induced by LPS, treatment with Ang-(1-7) was found to significantly suppress the serum concentrations of inflammatory cytokines TNF- α and IL-6 (Figure 4A and B). Similarly, Ang-(1-7) significantly inhibited the mRNA expression levels of TNF- α and IL-6 in the renal tissues of septic mice (Figure 4C and D). Furthermore, administration of Ang-(1-7) led to a significant reduction in BUN and Scr levels in septic mice (Figure 4E and F). Histopathological analysis revealed that septic mice exhibited swollen renal tubular epithelium, narrowed tubular lumens, dilated congested interstitial blood vessels, and extensive infiltration of inflammatory cells (Figure 4G and H). However, treated with Ang-(1-7) effectively alleviated the pathological alterations in septic mice (Figure 4G and H). These findings indicate that the occurrence of sepsis is associated with the activation of inflammatory cascades and renal injury. Meanwhile, Ang-(1-7) can suppress the inflammatory response in septic mice, alleviating acute kidney injury.

Ang-(1-7) Inhibited Glycolytic Levels and Ameliorated Mitochondrial Function in the Kidney of Septic Mice

In sepsis, energy metabolism shifts from OXPHOS to glycolysis. Western blot analysis revealed enhanced expression of glycolytic key enzymes PFKFB3 and PKM2 in the renal tissues of septic mice. Importantly, Ang-(1-7) significantly decreased the protein expression levels of PFKFB3 and PKM2 (Figure 5A–C). Furthermore, we refined the immunofluorescence analysis for PKM2, showing a significant decrease in PKM2 expression in the renal tissues of septic mice treated with Ang-(1-7) (Figure 5D and E). We also observed that Ang-(1-7) treatment significantly decreased the mRNA levels of HK2 in the renal tissues of septic mice (Figure 5F). Additionally, the serum lactate levels in septic mice markedly decreased after treatment with Ang-(1-7) (Figure 5G). These results indicate that Ang-(1-7) effectively suppresses enhanced glycolysis in septic mice.

The mitochondrion is the primary cellular organelle responsible for energy production. Alterations in mitochondrial structure and functional impairment can result in cellular damage within tissues. TEM analysis revealed severe mitochondrial swelling, loss of mitochondrial cristae, and vacuolar degeneration in the renal tubular epithelial cells of septic mice (Figure 5H and I). Ang-(1-7) effectively ameliorated mitochondrial cristae damage and mitochondrial swelling (Figure 5H and I). Mitochondrial structural impairment affects MMP, leading to a reduction in ATP levels. We observed that Ang-(1-7) treatment significantly increased the levels of MMP and ATP in the renal tissues of septic mice (Figure 5J and K). These findings indicate that mitochondrial function is inhibited under septic conditions, and Ang-(1-7) treatment effectively improves mitochondrial structure and function in septic mice, enhancing energy metabolism and thereby protecting against acute kidney injury induced by sepsis.

Ang-(1-7) Attenuated SLC25A1-HIF-1 α Expression in the Kidney of Septic Mice

We assessed the impact of Ang-(1-7) on the citrate metabolic pathway in LPS-induced septic mice. The Western blot analysis revealed enhanced expression of SLC25A1 protein in the renal tissues following LPS injection, however, Ang-(1-7) significantly downregulated the expression of this protein (Figure 6A and B). Similarly, immunofluorescence analysis demonstrated that Ang-(1-7) treatment effectively reduced the expression of SLC25A1 in the renal tissues of septic mice (Figure 6E and F). Moreover, in the renal tissues of septic mice, an upregulation in ACLY protein expression was noted, and this upregulation was effectively counteracted by Ang-(1-7) treatment (Figure 6A and C), suggesting that Ang-(1-7) may alleviate sepsis by inhibiting the expression of SLC25A1 in the citrate cycle pathway. HIF-1 α , a key regulator of glycolysis, was examined further. Western blot and immunofluorescence assays demonstrated that the levels of HIF-1 α were significantly lower in the renal tissues treated with Ang-(1-7) compared to septic mice (Figure 6A, D, G and H). The study demonstrates that Ang-(1-7) can inhibit the expression of key molecules in the citrate metabolic pathway, namely SLC25A1, ACLY, and HIF-1 α , suggesting a potential regulatory role of Ang-(1-7) in the Warburg effect through the citrate metabolic pathway, thereby modulating inflammation.

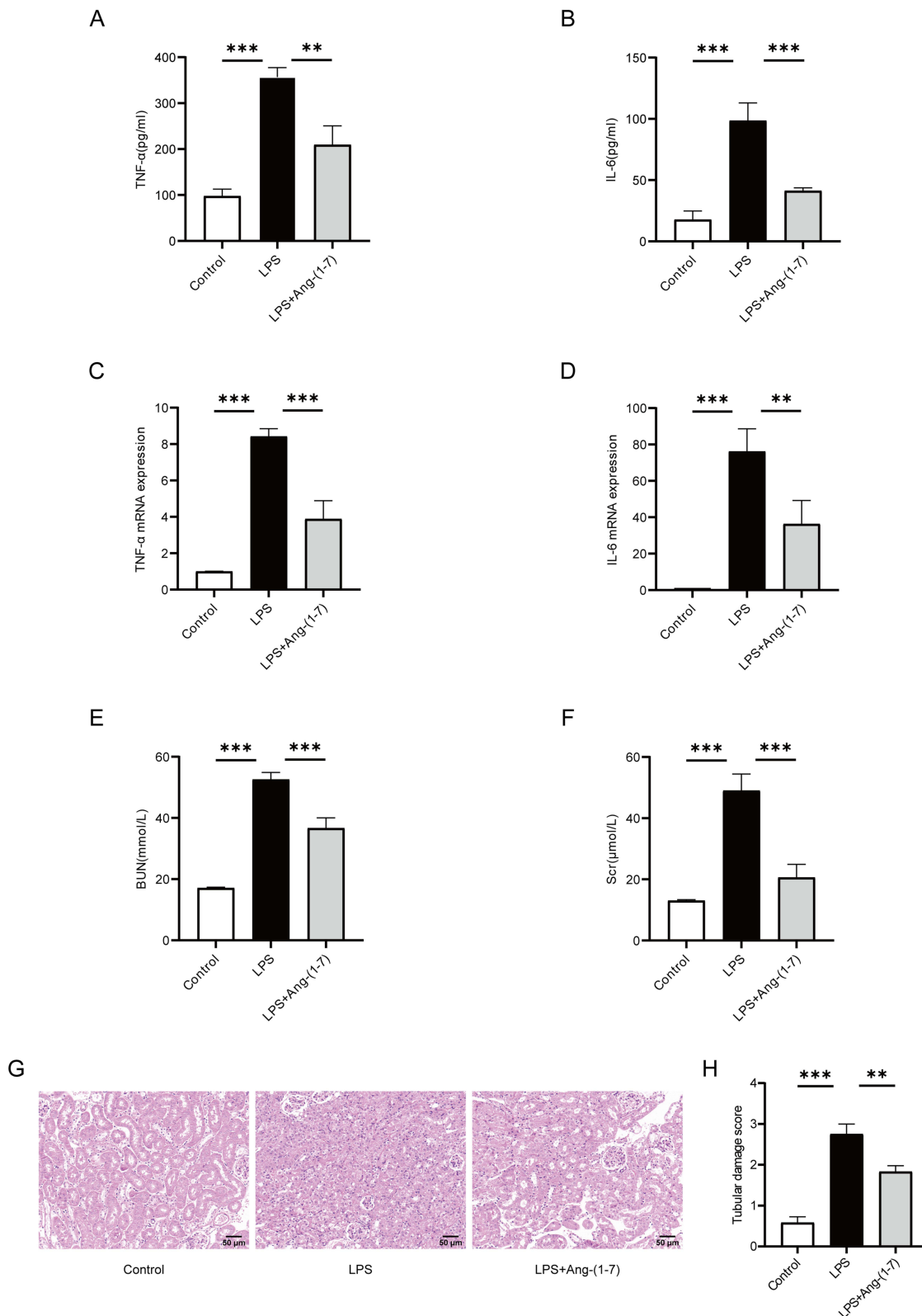


Figure 4 Ang-(1-7) inhibited the secretion of inflammatory factors in LPS-induced septic mice, and alleviated renal damage. **(A and B)** Levels of TNF- α and IL-6 in mouse serum were measured using the ELISA method. **(C and D)** Levels of TNF- α and IL-6 mRNA in mouse renal tissues were determined using qRT-PCR method. **(E and F)** Measurement of BUN and Scr levels in mice. **(G)** Representative images of renal tissues stained with HE ($\times 200$, scale bar: 50 μm). **(H)** Semi-quantitative scoring of renal tubular damage, based on the following criteria: 0, normal; 1, damage <25% of the area; 2, damage 25–50% of the area; 3, damage 50–75% of the area; and 4, damage >75% of the area. Error bars indicated the mean \pm SD for three separate experiments, ** $p < 0.01$, *** $p < 0.001$.

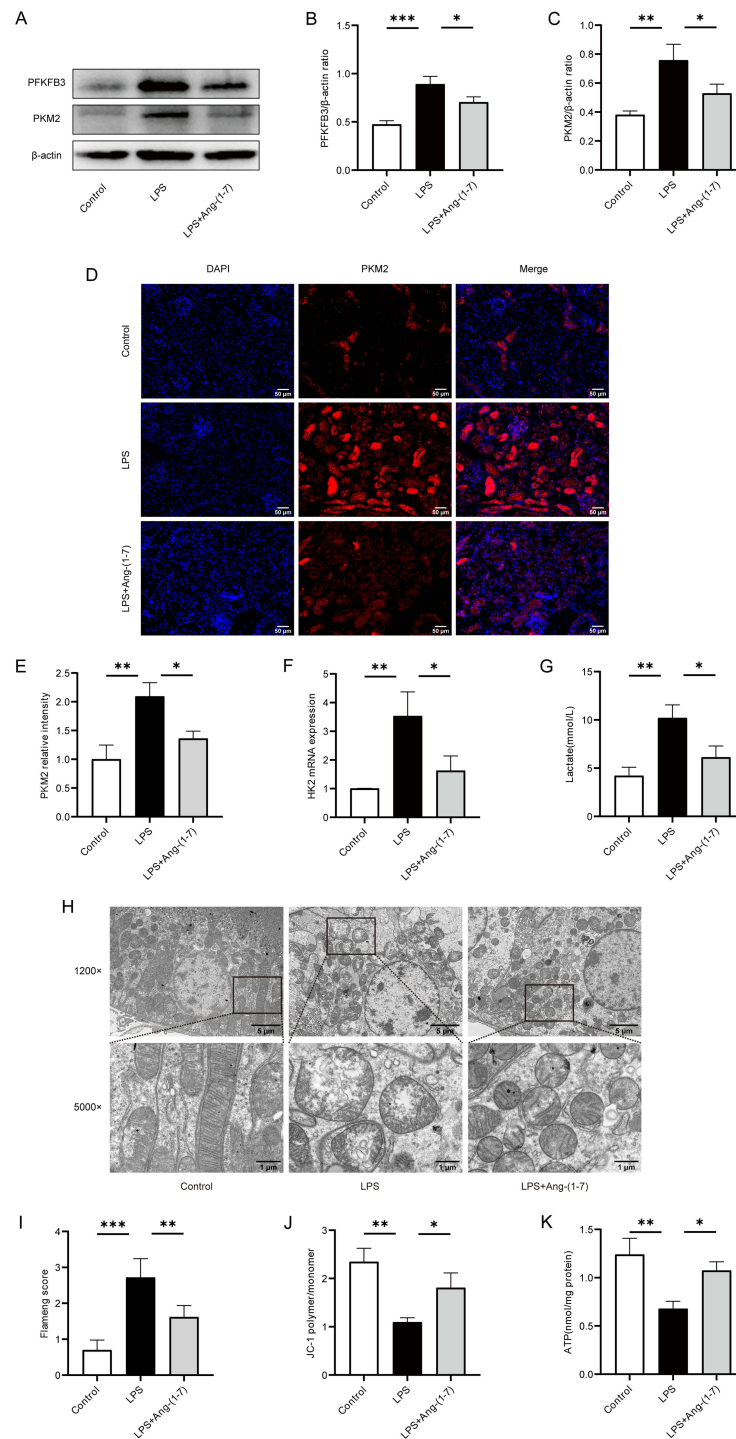


Figure 5 Ang-(1-7) inhibited LPS-induced sepsis-associated renal glycolysis and enhanced mitochondrial function in mice. **(A)** The protein expression levels of key glycolytic enzymes, PFKFB3 and PKM2, in renal tissues were assessed using Western blot analysis. **(B and C)** Quantification of protein concentrations of PFKFB3 and PKM2 was performed. **(D)** Representative immunofluorescence images of renal tissues PKM2 ($\times 200$, scale bar: 50 μm) were captured. **(E)** Analysis of the relative fluorescence intensity of PKM2. **(F)** Levels of HK2 in renal tissues were determined using qRT-PCR method. **(G)** Mouse serum lactate levels were measured using a lactate detection kit. **(H)** Representative transmission electron microscopy images of renal mitochondria were obtained. **(I)** Flaming score for mitochondrial injury, with the following scoring criteria: 0, normal; 1, mild swelling, decreased matrix density, and cristae separation; 2, mitochondrial swelling, transparent matrix, intact cristae; 3, severe swelling, matrix solidification, cristae rupture; 4, severe swelling with cristae rupture, complete disappearance of inner and outer membranes, forming a vacuole-like structure. **(J)** Renal tissues MMP levels were assessed by measuring the fluorescence intensity values of JC-1 polymer and monomer using a fluorescence microplate reader, and MMP levels were calculated. **(K)** ATP levels in mouse renal tissues were determined using an ATP detection kit. Error bars indicated the mean \pm SD for three separate experiments, * $p < 0.05$, ** $p < 0.01$, *** $p < 0.001$.

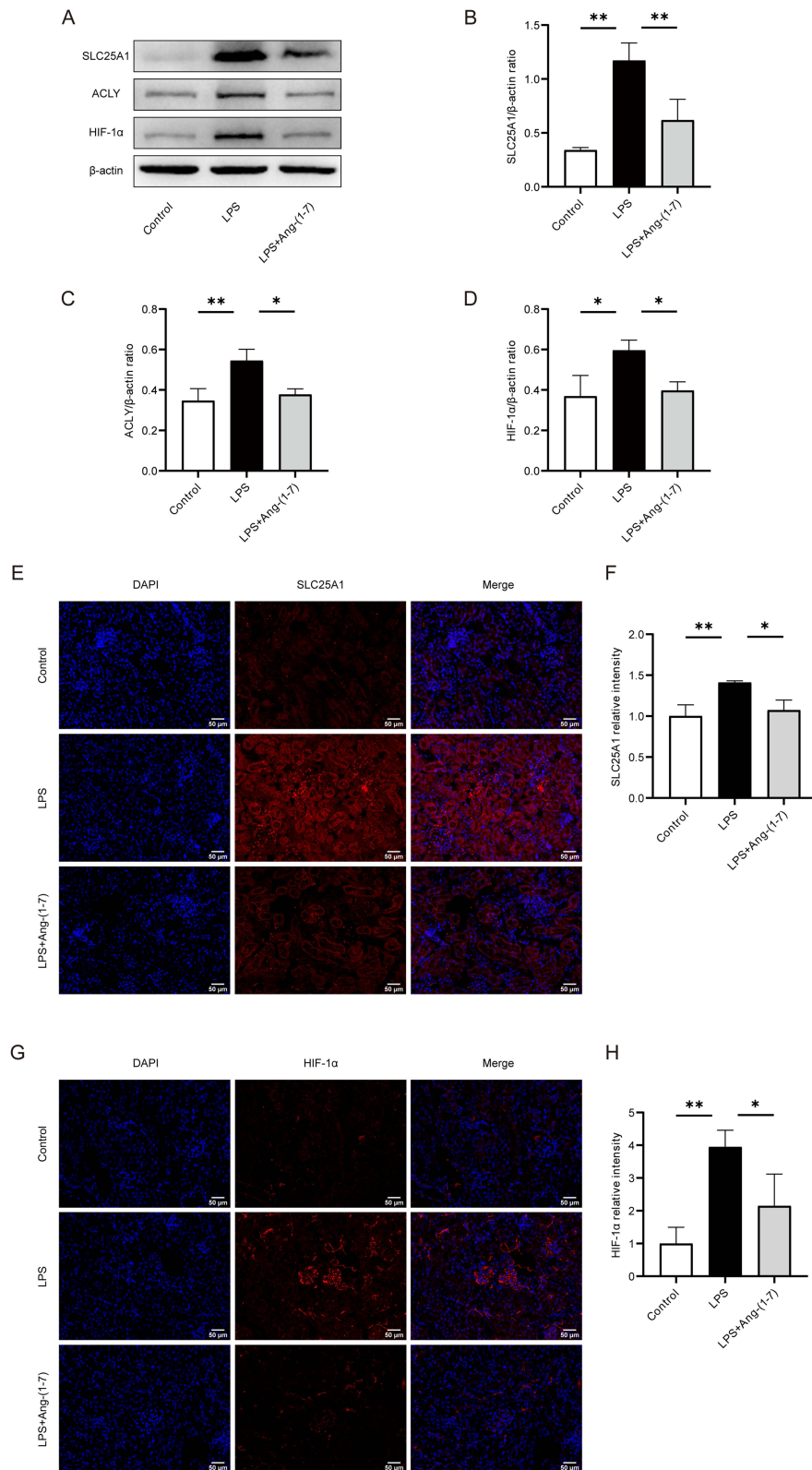


Figure 6 Ang-(1-7) inhibited citrate export pathway mediated by SLC25A1, ACLY, and HIF-1α in LPS-induced septic mice. **(A)** Western blot analysis was performed to evaluate the protein expression levels of SLC25A1, ACLY, and HIF-1α in mouse renal tissues. **(B–D)** Quantification of protein concentrations for SLC25A1, ACLY, and HIF-1α was carried out. **(E)** Representative immunofluorescence images of renal tissues SLC25A1 (×200, scale bar: 50 μm) are presented. **(F)** Analysis of the relative fluorescence intensity of SLC25A1. **(G)** Representative immunofluorescence images of renal tissues HIF-1α (×200, scale bar: 50 μm) are shown. **(H)** Analysis of the relative fluorescence intensity of HIF-1α. Error bars indicated the mean ± SD for three separate experiments, *p < 0.05, **p < 0.01.

Discussion

The essence of sepsis is a systemic uncontrolled inflammatory response. During the occurrence and progression of sepsis, various inflammatory mediators are excessively released, leading to widespread damage to the body's organs and ultimately resulting in septic shock and multiple organ dysfunction.²⁶ Macrophages play a crucial role in initiating and clearing pathogens, infected cells, dead cells, and cell debris in sepsis inflammation.²⁷ Activated macrophages demonstrate a rapid pro-inflammatory response in the initial stages of inflammation, known as M1 macrophages. M1 macrophages secrete a large amount of pro-inflammatory cytokines and chemokines, further recruiting more neutrophils, monocytes, and mast cells, thus amplifying the inflammatory response.²⁸ However, during the resolution phase, macrophages transition into M2 macrophages to resolve inflammation and repair damaged tissues.²⁹

The RAAS plays a significant role in the onset and progression of inflammation, affecting various organs and functions throughout the body. Formerly recognized as a key regulator of the cardiovascular system and electrolyte balance, further research has revealed its significant involvement in oxidative stress, metabolism, and inflammation.^{30,31} The RAAS is frequently activated during the process of organ damage induced by sepsis. This activation leads to an upregulation of the ACE/Ang II/AT1R axis, while the ACE2/Ang-(1-7)/MasR axis is downregulated.³² Angiotensin II (AngII) serves as a central carrier molecule in the classic RAAS and acts as a potent pro-inflammatory mediator.³³ Blood vessel tension converting enzyme 2 (ACE2) catalyzes the conversion of AngII to Ang-(1-7).³⁴ Ang-(1-7) functions as a biologically active small molecule, exerting its effects through specific binding to the Mas receptor. The Mas receptor selective antagonist A-779 can block a range of actions mediated by Ang-(1-7).^{22,35} Ang-(1-7) and AngII typically exhibit contrasting effects, thus Ang-(1-7) aids in counteracting inflammation. In our preliminary study, we found that Ang-(1-7), acting on the Mas receptor, regulates the expression of the macrophage TLR4 receptor under inflammatory conditions.²⁴ It inhibits the NF- κ B and MAPKs signaling pathways, suppresses the activation of M1-like macrophages, promotes the transformation of macrophages towards M2 polarization, and ameliorates the inflammatory damage in sepsis. Our current research, both in vivo and in vitro experiments, suggests that Ang-(1-7) can reduce the production of inflammatory factors TNF- α and IL-6. This is consistent with previous findings, indicating that Ang-(1-7) can improve the activation of macrophages and inflammation in septic mice. The key mechanism underlying the excessive activation of macrophages may be related to alterations in cellular metabolic patterns. In the inflammatory state, the metabolic features of macrophages include an increase in glycolytic flux and a reduction in mitochondrial OXPHOS. Enhanced glycolysis can lead to increased secretion of inflammatory cytokines and heightened phagocytic activity, ultimately contributing to heightened innate immune activation and worsened septic inflammation.³⁶ What is the anti-inflammatory mechanism of Ang-(1-7) in sepsis? Does it alleviate inflammation by improving the glycolysis and OXPHOS of macrophages, an immunometabolic pathway? Therefore, this study investigates the anti-inflammatory mechanism of Ang-(1-7) in sepsis by exploring the immunometabolic pathways. Given that the kidney are frequently affected organs in sepsis, with renal injury reflecting the prognosis of septic patients, and our previous research has observed that Ang-(1-7) can ameliorate renal injury in a hyperlipidemic state.^{37,38} Therefore, building upon prior research, this study utilized macrophages in an inflammatory state and septic mice as models, with the kidney of septic mice as the target organ, to investigate whether under inflammatory conditions, Ang-(1-7) exerts anti-inflammatory effects through intervening in glucose metabolism reprogramming and regulating the Warburg effect.

Inflammatory states induce metabolic changes in macrophages that resemble the Warburg effect. The Warburg effect describes the metabolic characteristic of tumors under normal oxygen conditions, where glycolysis remains dominant even under aerobic conditions capable of supporting oxidative metabolism.³⁹ And the pyruvate produced by the glycolytic pathway does not enter the TCA cycle and subsequent OXPHOS but is metabolized to lactate. Later research has found that the metabolism of innate immune cells is also similar to the Warburg effect, and this phenomenon has been observed in monocytes, macrophages, dendritic cells, and T cells.⁴⁰ When the Warburg effect occurs, activated macrophages no longer follow the metabolic pathway of the TCA cycle. Instead, they shift towards aerobic glycolysis, indicating a change in the glucose metabolism pattern characterized by increased glycolysis and reduced aerobic consumption. The majority of consumed glucose is converted to lactate, with minimal usage for OXPHOS.⁴¹ Simultaneously, the increased expression of key glycolytic enzymes such as HK2, PFKFB3, and PKM2 indicates heightened glycolytic activity.⁴²⁻⁴⁴ Our findings are consistent with this. Our in vitro experiments demonstrate that LPS-stimulated macrophages exhibit enhanced glycolysis,

undergoing the Warburg effect. Additionally, Ang-(1-7) downregulates the expression of glycolysis key enzymes HK2, PFKFB3, and PKM2 under inflammatory conditions, reducing lactate levels. This suggests that Ang-(1-7) can suppress the inflammatory response by alleviating the Warburg effect. Moreover, treatment with the Mas receptor antagonist A-779 can reverse the effects of Ang-(1-7), confirming that Ang-(1-7) exerts its actions through the Mas receptor. Recent research has indicated a potential improvement in mitigating organ damage in sepsis. Specifically, in cases of acute kidney injury induced by sepsis, the use of aerobic glycolysis inhibitor 2-deoxy-D-glucose (2-DG) has been shown to downregulate glycolysis, thereby ameliorating sepsis-induced kidney injury.⁴⁵ Our *in vivo* experiments in this study revealed an upregulation of key enzymes HK2, PFKFB3, and PKM2 in glycolysis, leading to the Warburg effect in sepsis-induced kidney injury. Building upon this, we further identified that Ang-(1-7) can protect septic mice from renal injury by inhibiting the Warburg effect, providing novel evidence for the role of Ang-(1-7) in alleviating sepsis through the regulation of the glycolytic pathway in glucose metabolism.

Mitochondria, as the primary energy source of living organisms, have been demonstrated as a central factor in regulating inflammation by providing energy to control it.^{46,47} Current research confirms that mitochondrial metabolites, oxidized through the TCA cycle in the mitochondrial matrix, utilize a series of complexes (I, II, III, IV, V) in the inner mitochondrial membrane to transfer electrons, generating ATP.⁴⁸ Changes in mitochondrial metabolism and physiological function, such as mitochondrial reactive oxygen species (mtROS), MMP, OXPHOS, ultrastructure, and the TCA cycle, are significant indicators of macrophage activation.⁴⁹ Mitochondria play a pivotal role in innate immune responses in various ways, serving as a focal point of inflammatory responses during bacterial infections or cellular injury, playing a crucial role in alleviating the inflammatory process.⁵⁰ Post pathogenic infections, mitochondrial dysfunction disrupts its dynamics and energetics, with many mitochondrial components and metabolites acting as damage-associated molecular patterns (DAMPs), exacerbating inflammation upon release into the cytoplasm or extracellular environment.^{50,51} Our findings demonstrate a significant reduction in mitochondrial complex I and III, as well as decreased MMP and ATP levels in macrophages stimulated by LPS. These findings demonstrate that under LPS stimulation, mitochondrial OXPHOS is suppressed and the capacity to produce ATP is decreased. However, Ang-(1-7) improves these levels, indicating that Ang-(1-7) can inhibit inflammation by modulating mitochondrial function. The regulation of mitochondrial function by Ang-(1-7) has also been confirmed in our *in vivo* experiments. In a septic mouse model, Ang-(1-7) was observed to enhance mitochondrial ultrastructure and restore MMP and ATP levels. Thus, Ang-(1-7) can inhibit the inflammatory state of sepsis by targeting mitochondrial dysfunction.

OXPHOS impairment is one manifestation of mitochondrial dysfunction, with interruptions in the TCA cycle being the cause of mitochondrial OXPHOS damage.⁵² Citrate accumulation serves as a pivotal point in the tricarboxylic acid cycle, and citrate export mediated by SLC25A1 establishes functional connections between mitochondrial oxidation and glycolysis. LPS stimulation results in the transportation of citrate by SLC25A1 into the cytoplasm, where it is converted to oxaloacetate and acetyl-CoA under the influence of ACLY.^{15,53} Interestingly, the transcription of genes encoding glycolytic enzymes HK2, PFK, and lactate dehydrogenase A (LDHA) is regulated downstream of ACLY.⁵⁴ Additionally, studies have revealed that the inhibition of the citrate metabolism pathway by downregulating SLC25A1 suppresses the expression of the transcription factor HIF-1 α , leading to weakened glycolysis and subsequent inflammation control.^{18,21} HIF-1 α is a common component in pathways regulating cellular metabolism and plays a role in modulating immune cell effector functions. HIF-1 α is induced in LPS-activated macrophages, enhancing the expression of glycolytic genes, thereby allowing sustained ATP production and also inducing the production of pro-inflammatory cytokines.^{21,55} The induction mechanism of HIF-1 α by LPS stimulation also involves succinate, which inhibits prolyl hydroxylases (PHDs), thereby promoting the switch to glycolysis and driving inflammation.⁵⁶ Thus, HIF-1 α is a key reprogramming process that promotes macrophage metabolism in an inflammatory state. Our *in vivo* and *in vitro* experiments indicate that Ang-(1-7) can reduce the enhanced SLC25A1, ACLY, and HIF1 α in an inflammatory state. Furthermore, *in vitro* experiments have also found that Ang-(1-7) can reduce the accumulation of TCA cycle intermediate citrate in macrophages, suggesting that Ang-(1-7) may improve inflammation by regulating the Warburg effect through modulation of the citrate pathway. Our research findings provide a promising new direction for the study of how Ang-(1-7) alleviates aerobic glycolysis and mitochondrial damage in activated macrophages and septic mice.

However, our study still has some limitations. We inferred that Ang-(1-7) may regulate the Warburg effect through the citrate pathway mediated by SLC25A1 to inhibit inflammation. Nevertheless, we only selected key molecules in the detection process and did not cover all molecules in the entire response and other possible signaling pathways. Secondly, our in vitro and in vivo experiments suggest that Ang-(1-7) is a potential target for alleviating sepsis, but this strategy requires further investigation.

Conclusion

Our research indicates that in the LPS-induced macrophage and septic mice, Ang-(1-7) can regulate the SLC25A1-driven citrate pathway, inhibit glycolysis, and restore mitochondrial damage, thereby reducing inflammation. However, more experiments are needed to explore the deeper mechanisms of Ang-(1-7) in regulating immune metabolism. In conclusion, Ang-(1-7) may serve as a potential candidate target for metabolic reprogramming, and the study findings suggest a target for intervening in acute inflammation by regulating the Warburg effect in immune cells.

Acknowledgments

This study was supported by the National Natural Science Foundation of China (81771738), Chongqing Science and Technology Innovation Leading Talent Support Program (CQYC202104), the Program for Youth Innovation in Future Medicine, Chongqing Medical University (W0197) and the Kuanren Talents Program of the Second Affiliated Hospital of Chongqing Medical University (13-002-017).

Disclosure

The authors report no conflicts of interest in this work.

References

- Cecconi M, Evans L, Levy M, Rhodes A. Sepsis and septic shock. *Lancet*. 2018;392(10141):75–87. doi:10.1016/S0140-6736(18)30696-2
- Venet F, Monneret G. Advances in the understanding and treatment of sepsis-induced immunosuppression. *Nat Rev Nephrol*. 2018;14(2):121–137. doi:10.1038/nrneph.2017.165
- Chen XS, Liu YC, Gao YL, Shou ST, Chai YF. The roles of macrophage polarization in the host immune response to sepsis. *Int Immunopharmacol*. 2021;96:11. doi:10.1016/j.intimp.2021.107791
- Liu PS, Wang HP, Li XY, et al. alpha-ketoglutarate orchestrates macrophage activation through metabolic and epigenetic reprogramming. *Nat Immunol*. 2017;18(9):985–994. doi:10.1038/ni.3796
- Krawczyk CM, Holowka T, Sun J, et al. Toll-like receptor-induced changes in glycolytic metabolism regulate dendritic cell activation. *Blood*. 2010;115(23):4742–4749. doi:10.1182/blood-2009-10-249540
- Nonnenmacher Y, Hiller K. Biochemistry of proinflammatory macrophage activation. *Cell Mol Life Sci*. 2018;75(12):2093–2109.
- Rodríguez-Prados JC, Través PG, Cuenca J, et al. Substrate fate in activated macrophages: a comparison between innate, classic, and alternative activation. *J Immunol*. 2010;185(1):605–614. doi:10.4049/jimmunol.0901698
- Través PG, de Atauri P, Marin S, et al. Relevance of the MEK/ERK signaling pathway in the metabolism of activated macrophages: a metabolomic approach. *J Immunol*. 2012;188(3):1402–1410.
- Palsson-McDermott EM, Curtis AM, Goel G, et al. Pyruvate Kinase M2 regulates hif-1 alpha Activity and IL-1 beta induction and is a critical determinant of the Warburg effect in LPS-activated macrophages. *Cell Metab*. 2015;21(1):65–80. doi:10.1016/j.cmet.2014.12.005
- Kelly B, O'Neill LAJ. Metabolic reprogramming in macrophages and dendritic cells in innate immunity. *Cell Res*. 2015;25(7):771–784. doi:10.1038/cr.2015.68
- Paggio A, Checchetto V, Campo A, et al. Identification of an ATP-sensitive potassium channel in mitochondria. *Nature*. 2019;572(7771):609–613. doi:10.1038/s41586-019-1498-3
- O'Neill LAJ. A Broken Krebs Cycle in Macrophages. *Immunity*. 2015;42(3):393–394. doi:10.1016/j.immuni.2015.02.017
- Williams NC, O'Neill LAJ. A role for the Krebs cycle intermediate citrate in metabolic reprogramming in innate immunity and inflammation. *Front Immunol*. 2018;9:11. doi:10.3389/fimmu.2018.00141
- Infantino V, Convertini P, Cucci L, et al. ACCELERATED PUBLICATION The mitochondrial citrate carrier: a new player in inflammation. *Biochem J*. 2011;438:433–436. doi:10.1042/BJ20111275
- Santarsiero A, Convertini P, Todisco S, et al. ACLY Nuclear Translocation in Human Macrophages Drives Proinflammatory Gene Expression by NF-kappa B Acetylation. *Cells*. 2021;10(11):21. doi:10.3390/cells10112962
- Lauterbach MA, Hanke JE, Serefidou M, et al. Toll-like Receptor Signaling Rewires Macrophage Metabolism and Promotes Histone Acetylation via ATP-Citrate Lyase. *Immunity*. 2019;51(6):997–1011.e7. doi:10.1016/j.immuni.2019.11.009
- Chen Q, Cui K, Zhao ZQ, et al. LPS stimulation stabilizes HIF-1 alpha by enhancing HIF-1 alpha acetylation via the PARP1-SIRT1 and ACLY-Tip60 pathways in macrophages. *FASEB J*. 2022;36(7):16. doi:10.1096/fj.202200256R
- Li Y, Li YC, Liu XT, et al. Blockage of citrate export prevents TCA cycle fragmentation via Irg1 inactivation. *Cell Rep*. 2022;38(7):25. doi:10.1016/j.celrep.2022.110391
- Tennant DA. PK-M2 Makes Cells Sweeter on HIF1. *Cell*. 2011;145(5):647–649. doi:10.1016/j.cell.2011.05.009

20. Saldana-Caboverde A, Nissanka N, Garcia S, Lombes A, Diaz F. Hypoxia promotes mitochondrial complex I abundance via HIF-1 alpha in Complex III and Complex IV Deficient Cells. *Cells*. 2020;9(10):29. doi:10.3390/cells9102197
21. Corcoran SE, O'Neill LAJ. HIF1 alpha and metabolic reprogramming in inflammation. *J Clin Invest*. 2016;126(10):3699–3707. doi:10.1172/JCI84431
22. Santos RAS, Silva A, Maric C, et al. Angiotensin-(1-7) is an endogenous ligand for the G protein-coupled receptor Mas. *Proc Natl Acad Sci U S A*. 2003;100(14):8258–8263. doi:10.1073/pnas.1432869100
23. Santos RAS, Sampaio WO, Alzamora AC, et al. THE ACE2/ANGIOTENSIN-(1-7)/MAS AXIS OF THE RENIN-ANGIOTENSIN SYSTEM: FOCUS ON ANGIOTENSIN-(1-7). *Physiol Rev*. 2018;98(1):505–553. doi:10.1152/physrev.00023.2016
24. Pan H, Huang WH, Wang ZJ, et al. The ACE2-Ang-(1-7)-Mas Axis Modulates M1/M2 Macrophage Polarization to Relieve CLP-Induced Inflammation via TLR4-Mediated NF-kappa b and MAPK Pathways. *J Inflamm Res*. 2021;14:2045–2060. doi:10.2147/JIR.S307801
25. Poston JT, Koyner JL. Sepsis associated acute kidney injury. *BMJ*. 2019;364:17.
26. Singer M, Deutschman CS, Seymour CW, et al. The third international consensus definitions for sepsis and septic shock (Sepsis-3). *J Am Med Assoc*. 2016;315(8):801–810. doi:10.1001/jama.2016.0287
27. Shapouri-Moghaddam A, Mohammadian S, Vazini H, et al. Macrophage plasticity, polarization, and function in health and disease. *J Cell Physiol*. 2018;233(9):6425–6440. doi:10.1002/jcp.26429
28. Locati M, Curtale G, Mantovani A. Diversity, Mechanisms, and Significance of Macrophage Plasticity. In: Abbas AK, Aster JC, Feany MB, editors. *Annual Review of Pathology: Mechanisms of Disease*. Palo Alto: Annual Reviews; 2020:123–147.
29. Liu YC, Zou XB, Chai YF, Yao YM. Macrophage polarization in inflammatory diseases. *Int J Biol Sci*. 2014;10(5):520–529. doi:10.7150/ijbs.8879
30. Te Riet L, Van Esch JHM, Roks AJM, Van Den Meiracker AH, Danser AHJ. Hypertension renin-angiotensin-aldosterone system alterations. *CircRes*. 2015;116(6):960–975.
31. Colafella KMM, Bovee DM, Danser AHJ. The renin-angiotensin-aldosterone system and its therapeutic targets. *Exp Eye Res*. 2019;186:7.
32. Chen QH, Liu JJ, Wang WQ, et al. Sini decoction ameliorates sepsis-induced acute lung injury via regulating ACE2-Ang (1-7)-Mas axis and inhibiting the MAPK signaling pathway. *Biomed Pharmacother*. 2019;115:12. doi:10.1016/j.biopha.2019.108971
33. Tsai HJ, Liao MH, Shih CC, Ka SM, Tsao CM, Wu CC. Angiotensin-(1-7) attenuates organ injury and mortality in rats with polymicrobial sepsis. *Crit Care*. 2018;22:10. doi:10.1186/s13054-018-2210-y
34. Passos-Silva DG, Verano-Braga T, Santos RAS. Angiotensin-(1-7): beyond the cardio-renal actions. *Clin Sci*. 2013;124(7–8):443–456. doi:10.1042/CS20120461
35. Santos RAS, Ferreira AJ, Verano-Braga T, Bader M. Angiotensin-converting enzyme 2, angiotensin-(1-7) and Mas: new players of the renin-angiotensin system. *J Endocrinol*. 2013;216(2):R1–R17. doi:10.1530/JOE-12-0341
36. Liu Y, Xu RY, Gu HY, et al. Metabolic reprogramming in macrophage responses. *Biomark Res*. 2021;9(1):17. doi:10.1186/s40364-020-00251-y
37. Huang WH, Tang L, Cai Y, Zheng YN, Zhang L. Effect and mechanism of the Ang-(1-7) on human mesangial cells injury induced by low density lipoprotein. *Biochem Biophys Res Commun*. 2014;450(2):1051–1057. doi:10.1016/j.bbrc.2014.06.107
38. Zheng YN, Tang L, Huang WH, et al. Anti-Inflammatory Effects of Ang-(1-7) in Ameliorating HFD-Induced Renal Injury through LDLr-SREBP2-SCAP Pathway. *PLoS One*. 2015;10(8):18. doi:10.1371/journal.pone.0136187
39. Warburg O, Wind F, Negelein E. THE METABOLISM OF TUMORS IN THE BODY. *J Gener Physiol*. 1927;8(6):519–530. doi:10.1085/jgp.8.6.519
40. Palsson-McDermott EM, O'Neill LAJ. The Warburg effect then and now: from cancer to inflammatory diseases. *Bioessays*. 2013;35(11):965–973. doi:10.1002/bies.201300084
41. Zhu LN, Zhao QJ, Yang T, Ding WJ, Zhao Y. Cellular Metabolism and Macrophage Functional Polarization. *Int Rev Immunol*. 2015;34(1):82–100. doi:10.3109/08830185.2014.969421
42. Yuan Y, Fan GJ, Liu YQ, et al. The transcription factor KLF14 regulates macrophage glycolysis and immune function by inhibiting HK2 in sepsis. *Cell Mol Immunol*. 2022;19(4):504–515. doi:10.1038/s41423-021-00806-5
43. Yuan YF, Wang W, Zhang Y, et al. Apelin-13 Attenuates Lipopolysaccharide-Induced Inflammatory Responses and Acute Lung Injury by Regulating PFKFB3-Driven Glycolysis Induced by NOX4-Dependent ROS. *J Inflamm Res*. 2022;15:2121–2139. doi:10.2147/JIR.S348850
44. Ying ZH, Li HM, Yu WY, Yu CH. Iridin Prevented Against Lipopolysaccharide-Induced Inflammatory Responses of Macrophages via Inactivation of PKM2-Mediated Glycolytic Pathways. *J Inflamm Res*. 2021;14:341–354. doi:10.2147/JIR.S292244
45. Tan CY, Gu J, Li T, et al. Inhibition of aerobic glycolysis alleviates sepsis-induced acute kidney injury by promoting lactate/Sirtuin 3/AMPK-regulated autophagy. *Int J Mol Med*. 2021;47(3):12. doi:10.3892/ijmm.2021.4852
46. Harrington JS, Ryter SW, Plataki M, Price DR, Choi AMK. Mitochondria in health, disease, and aging. *Physiol Rev*. 2023;103(4):2349–2422. doi:10.1152/physrev.00058.2021
47. Vringer E, Tait SWG. Mitochondria and cell death-associated inflammation. *Cell Death Differ*. 2023;30(2):304–312. doi:10.1038/s41418-022-01094-w
48. Yin M, O'Neill LAJ. The role of the electron transport chain in immunity. *FASEB J*. 2021;35(12):13. doi:10.1096/fj.202101161R
49. Van den Bossche J, Baardman J, Otto NA, et al. Mitochondrial Dysfunction Prevents Repolarization of Inflammatory Macrophages. *Cell Rep*. 2016;17(3):684–696. doi:10.1016/j.celrep.2016.09.008
50. Marchi S, Guilbaud E, Tait SWG, Yamazaki T, Galluzzi L. Mitochondrial control of inflammation. *Nat Rev Immunol*. 2023;23(3):159–173.
51. Andrieux P, Chevillard C, Cunha-Neto E, Nunes JPS. Mitochondria as a Cellular Hub in Infection and Inflammation. *Int J Mol Sci*. 2021;22(21):29. doi:10.3390/ijms222111338
52. Strelko CL, Lu WY, Dufort FJ, et al. Itaconic Acid Is a Mammalian Metabolite Induced during Macrophage Activation. *J Am Chem Soc*. 2011;133(41):16386–16389. doi:10.1021/ja2070889
53. Williams NC, O'Neill LA. ACLY-matizing Macrophages to Histone Methylation curcine Immunometabolic Reprogramming. *Trends Immunol*. 2020;41(2):93–94.
54. Wellen KE, Hatzivassiliou G, Sachdeva UM, Bui TV, Cross JR, Thompson CB. ATP-Citrate Lyase Links Cellular Metabolism to Histone Acetylation. *Science*. 2009;324(5930):1076–1080. doi:10.1126/science.1164097
55. Zhong WJ, Liu T, Yang HH, et al. TREM-1 governs NLRP3 inflammasome activation of macrophages by firing up glycolysis in acute lung injury. *Int J Biol Sci*. 2023;19(1):242–257. doi:10.7150/ijbs.77304
56. Tannahill GM, Curtis AM, Adamik J, et al. Succinate is an inflammatory signal that induces IL-1 beta through HIF-1 alpha. *Nature*. 2013;496(7444):238. doi:10.1038/nature11986

Journal of Inflammation Research

Dovepress

Publish your work in this journal

The Journal of Inflammation Research is an international, peer-reviewed open-access journal that welcomes laboratory and clinical findings on the molecular basis, cell biology and pharmacology of inflammation including original research, reviews, symposium reports, hypothesis formation and commentaries on: acute/chronic inflammation; mediators of inflammation; cellular processes; molecular mechanisms; pharmacology and novel anti-inflammatory drugs; clinical conditions involving inflammation. The manuscript management system is completely online and includes a very quick and fair peer-review system. Visit <http://www.dovepress.com/testimonials.php> to read real quotes from published authors.

Submit your manuscript here: <https://www.dovepress.com/journal-of-inflammation-research-journal>